Enhanced absorption of waves in stealth hyperuniform disordered media

FLORIAN BIGOURDAN,[1] ROMAIN PIERRAT,[1,2] AND RÉMI CARMINATI[1,3]

[1]*Institut Langevin, ESPCI Paris, CNRS, PSL University, 1 rue Jussieu, 75005 Paris, France*
[2]*romain.pierrat@espci.fr*
[3]*remi.carminati@espci.fr*

Abstract: We study the propagation of waves in a set of absorbing subwavelength scatterers positioned on a stealth hyperuniform point pattern. We show that spatial correlations in the disorder substantially enhance absorption compared to a fully disordered structure with the same density of scatterers. The non-resonant nature of the mechanism provides broad angular and spectral robustness. These results demonstrate the possibility to design low-density materials with blackbody-like absorption.

1. Introduction

Enhancing the absorption of waves is of paramount importance in a number of applications, including solar heating [1], photovoltaics [2], molecular spectroscopy and sensing [3], acoustic insulation [4,5], seismology [6], or ocean waves [7]. In optics, perfect absorption of coherent light has been demonstrated long-ago on designed periodic structures supporting surface plasmons [8]. The conception of metallic nanostructures to enhance absorption has become a strategy to increase the efficiency of photovoltaic conversion or photodetection of visible or near infrared light, taking advantage of the broadband nature of plasmon resonances. A drawback is the strong absorption in the metal itself, which reduces the absorption enhancement in the region of interest (e.g., the active semiconductor). Optimized nanostructures also require costly nanofabrication techniques, and can be highly sensitive to imperfections. The concept of coherent perfect absorption (CPA) has been generalized, showing that total absorption at a given frequency can be reached in any absorbing material provided that the incident wavefront has been spatially shaped to match an absorption eigenmode [9, 10]. Coupled to wavefront shaping techniques, CPA permits total absorption of light in complex disordered media [11–13]. An important difference between Refs. [9, 10] and [11–13] is that the former are based on resonant absorption by an eigenmode at certain frequency. However, the latter are based on non-resonant coupling of light into an eigenchannel that can occur over a continuous frequency range and its enhancement effect can be broadband. Nevertheless, resonant absorption in designed nanostructures and CPA both require a coherent (shaped or unshaped) incident wavefront. This makes the absorption process sensitive to changes in the incident wave (direction, polarization and to a lesser extend spectrum), or to a reduction of its degree of coherence, thus limiting the range of targeted applications.

Alternatively, absorption of natural light in disordered materials has been put forward recently, mostly in the context of photovoltaics [14–17]. It has been known for long that structural correlations (e.g., correlations in the positions of scatterers dispersed in a homogeneous medium) have a strong impact on the scattering properties [18–25]. The possibility to increase absorption using correlated disorder has been demonstrated in thin films patterned with holes [26], and put forward recently in particular cases [27–30]. Nevertheless, a general strategy to optimize disordered materials in terms of their ability to absorb light (and more generally waves) over a broad spectral and angular range is still missing.

Previous works were often guided by the idea of increasing the optical path length [15, 16], or

based on an optimization process without targeting a particular physical mechanism [11–13, 17]. In this manuscript, we propose an alternative strategy. First, we demonstrate the existence of an upper bound for the absorbed power, and discuss the underlying physical picture. This picture naturally dictates a methodology to enhance absorption in a disordered medium by suppressing scattering using structural correlations, and maximizing the absorbance in the resulting effective homogeneous medium. Second, based on numerical simulations, we show that hyperuniform materials, a specific class of correlated disordered materials, permit to reach an absorption level close to the predicted upper bound, with substantial spectral and angular robustness. The results demonstrate the substantial impact of structural correlations on absorption, offering the possibility to design low-density disordered materials with blackbody-like absorption.

2. Upper bound for wave absorption in disordered media

Upper bounds for the absorbed power in photonic materials have been discussed in previous studies. One of them applies to materials made of discrete scatterers with a fixed position in space, the degree of freedom being the polarizabilities of the individual scatterers [31]. Since in the present work we focus on the degrees of freedom offered by the spatial distribution of scatterers, this upper bound is not directly applicable. Another upper bound was derived for a medium with given material properties (dielectric function) and a tunable geometry [32]. Since our objective is to define strategies to optimize the absorption in a disordered medium described statistically, we propose another approach to derive an upper bound that directly applies to the statistically averaged absorbed power. As we will see, this upper bound derivation gives insight for the definition of strategies to reach this bound [i.e. to optimize the level of absorption by designing the statistical properties (spatial correlations) of the disordered medium].

Let us consider a disordered medium embedded in a volume V with external surface S, illuminated by a monochromatic incident electric field with complex amplitude $\mathbf{E}_0$. From Poynting's theorem, and writing the total field $\mathbf{E} = \mathbf{E}_0 + \mathbf{E}_s$ with $\mathbf{E}_s$ the scattered field, energy consevation can be written in the form $P_e = P_a + P_s$ [33]. In this expression, $P_e = \mathrm{Re} \int_V \mathbf{j} \cdot \mathbf{E}_0^* \mathrm{d}^3 r / 2$ is the extinction power, $\mathbf{j}$ being the induced current density in volume V, $P_a = \mathrm{Re} \int_V \mathbf{j} \cdot \mathbf{E}^* \mathrm{d}^3 r / 2$ is the absorbed power, and $P_s = \mathrm{Re} \oint_S (\mathbf{E}_s \times \mathbf{H}_s^*) \cdot \mathbf{n}_S \mathrm{d}^2 r / 2$ is the scattered power, $\mathbf{H}_s$ being the scattered magnetic field and $\mathbf{n}_S$ the outward normal on S. Since we are interested in a statistical description of the disordered medium, we introduce the ensemble average denoted by $\langle \cdots \rangle$, and write the fields and current density as a sum of an average value and a fluctuating part: $\mathbf{X} = \langle \mathbf{X} \rangle + \delta \mathbf{X}$ with $\mathbf{X} \in \{\mathbf{E}, \mathbf{E}_s, \mathbf{H}_s, \mathbf{j}\}$ (note that $\langle \delta \mathbf{X} \rangle = 0$, and that $\mathbf{E}_0 = \langle \mathbf{E}_0 \rangle$ since $\mathbf{E}_0$ is deterministic). Introducing these expansions into the expressions of the extinction, absorbed and scattered powers, they can be cast in the form $\langle P \rangle = \overline{P} + \widetilde{P}$, where $\overline{P}$ is the component involving average quantities $\langle \mathbf{X} \rangle$ and $\widetilde{P}$ the component involving fluctuations $\delta \mathbf{X}$ (see App. A). Noting that $\langle P_e \rangle = \overline{P}_e$, energy conservation becomes on average $\overline{P}_e = \overline{P}_a + \widetilde{P}_a + \overline{P}_s + \widetilde{P}_s$. An important result of multiple scattering theory states that the averaged field obeys a wave equation in an effective homogeneous medium [34, 35]. Energy conservation for the averaged field can be written $\overline{P}_e = \overline{P}_a + \overline{P}_s$ (see App. A). Combining the two preceding equations leads to $\widetilde{P}_a + \widetilde{P}_s = 0$. As a result, the averaged absorbed power can be written

$$\langle P_a \rangle = \overline{P}_a - \widetilde{P}_s. \tag{1}$$

Note that $\widetilde{P}_s \geq 0$ since it can be reduced to the integration of $|\delta \mathbf{E}_s|^2$ over a closed-surface encompassing the medium in the far field. For the sake of simplicity, we now assume that the medium is a slab of finite thickness and illuminated by a plane-wave $\mathbf{E}_0$ which will be the situation of interest in the following. We consider the volume V to be a portion of the slab with cross section Σ. In that simple case, the power $\overline{P}_a$ absorbed in the effective homogeneous medium (as seen by the averaged field) cannot exceed the incident power $P_0 = \int_\Sigma \mathbf{\Pi}_0 \cdot \mathbf{n}_\Sigma \mathrm{d}^2 r$ where $\mathbf{\Pi}_0$ is the

incident Poynting vector and $\mathbf{n}_\Sigma$ the inward normal on Σ. We finally have

$$\langle P_a \rangle \leq P_0 - \widetilde{P}_s. \tag{2}$$

The derivation of this upper bound for the averaged absorbed power in a disordered medium embedded in a slab geometry is the first result in this article.

This upper bound suggests three strategies to increase the absorbed power: (1) Inhibit $\widetilde{P}_s$ while keeping $\overline{P}_a$ approximately constant, (2) for a fixed $\widetilde{P}_s$, maximize $\overline{P}_a$ as close as possible to P_0, or (3) inhibit $\widetilde{P}_s$ and maximize $\overline{P}_a$. Strictly speaking, finding the statistical classes of disorder that maximize the absorbed power is challenging. Indeed, $\overline{P}_a$ and $\widetilde{P}_s$ depend on transport parameters such as the effective refractive index and the scattering and absorption mean free paths, that have a complex dependence on the structural correlations of disorder [36]. In the following we will constrain the problem by considering media made of absorbing discrete scatterers dispersed in a transparent background, and characterized statistically by the spatial correlation in the positions of the scatterers. Furthermore, we will consider the special class of stealth hyperuniform disorder, that is known to produce $\widetilde{P}_s \ll P_0$ for large wavelengths even in dense materials [24]. In particular, a key question that we will address below concerns the validity of the preceding inequality in the presence of strong absorption.

3. Wave absorption in hyperuniform materials

Hyperuniform point patterns are such that the variance of the number of points within a sphere of radius R increases slower than the average number of points when R tends to infinity [37]. For a set of N points with positions $\mathbf{r}_j$, this property is equivalent to saying that the structure factor

$$S(\mathbf{q}) = \frac{1}{N} \left| \sum_{j=1}^{N} \exp[i\mathbf{q} \cdot \mathbf{r}_j] \right|^2 \tag{3}$$

vanishes when $|\mathbf{q}| \to 0$. First introduced for their interest in close packing processes [37], hyperuniform distributions of scatterers (hereafter denoted by hyperuniform materials) also produce materials of interest in wave physics, in particular due to their ability to produce bandgaps even in absence of periodicity [38–44]. Stealth hyperuniform materials is a specific class for which $S(\mathbf{q})$ strictly vanishes on a domain Ω of typical size K around $\mathbf{q} = 0$ [45, 46]. The size K actually controls the degree of spatial correlations. For large K, the system is very constrained, generating short and long-range order. For $K \to 0$, structural correlations are relaxed and the system tends to a fully disordered material. The degree of order in the pattern is usually measured by the ratio $\chi = [K/(2\pi)]^d/(2d\rho)$, with ρ the density of points and d the dimension of space. χ has to be understood as the number of constrained degrees of freedom (DOF) normalized by the total number of DOF. $\chi = 0$ corresponds to an uncorrelated pattern (fully disordered structure without any constraints), while $\chi = 1$ characterizes a perfect crystal with infinite range correlations [45].

In the single-scattering regime, the scattered intensity is directly proportionnal to the structure factor $S(\mathbf{q})$, with $\mathbf{q} = \mathbf{k}_s - \mathbf{k}_i$, $\mathbf{k}_s$ and $\mathbf{k}_i$ being the scattered and incident wavevectors. A stealth hyperuniform material does not scatter light for wavelengths satisfying $\lambda > 8\pi/K$, which corresponds to scattering wavevectors $\mathbf{q}$ lying in the domain Ω [24]. In the multiple-scattering regime, transparency also holds for large λ, provided that the effective scattering mean-free path ℓ_s^H is larger than the system size L [24] (we use the superscript H for quantities characterizing the hyperuniform material). In this regime, we have $\widetilde{P}_s^H \ll P_0$, leading us to the idea that hyperuniform materials made with absorbing scatterers could be used to optimize the absorbed power, along the line denoted by strategy (1) above.

In order to support this idea, we present numerical simulations of wave scattering in two-dimensional model materials made of subwavelength electric-dipole scatterers distributed on a

stealth hyperuniform point pattern. To proceed, we generate 60 configurations with thickness L and transverse size $3L$, following the algorithm in Ref. [45] (also described in Ref. [24]). A value $\chi = 0.44$ is chosen, permitting to simulate large systems with a limited number of scatterers, although the behaviors discussed below are also observed for smaller values of χ. The value $\chi = 0$ has also been chosen to make a comparison with a fully disordered (uncorrelated) structure. In that case, the system is simply generated by picking-up random positions of the scatterers uniformly in the volume $L \times 3L$. For simplicity we consider electromagnetic waves with an electric field perpendicular to the plane containing the scatterers. Each scatterer is described by its electric polarizability $\alpha(\omega) = -4\eta c^2/[Q(\omega^2 - \omega_0^2) + i\omega^2]$. Here c is the speed of light in vacuum, ω_0 is the resonance frequency, $Q = \omega_0/\Gamma$ is the quality factor, $\Gamma = \Gamma_R + \Gamma_{NR}$ is the linewidth, with a radiative and a non-radiative contribution (absorption), and $\eta = \Gamma_R/\Gamma$ is the quantum efficiency (or albedo). From the polarizability, we can deduce the scattering cross-section $\sigma_s = k_0^3|\alpha(\omega)|^2/4$, the extinction cross-section $\sigma_e = k_0 \operatorname{Im}[\alpha(\omega)]$ and the absorption cross-section $\sigma_a = \sigma_e - \sigma_s$ of the scatterers, with $k_0 = \omega/c = 2\pi/\lambda$ the wavenumber in vacuum. Given a number density ρ of scatterers, we introduce as references the scattering and absorption mean-free paths in the independent scattering approximation (ISA, also known as Boltzmann approximation), defined as $\ell_s^B = (\rho\sigma_s)^{-1}$ and $\ell_a^B = (\rho\sigma_a)^{-1}$. The disordered medium is illuminated from the left by a plane-wave at normal incidence (as shown schematically in the inset in Fig. 1). Maxwell's equations are solved using the coupled-dipoles method [47], and once the electric field illuminating each scatterer is known, the total absorbed power P_a^H is readily calculated (see App. B for more details on the numerical procedure). Repeating the calculation on the set of generated configurations, an ensemble average is performed to obtain $\langle P_a^H \rangle$. Running the same simulations on a set of configurations with uncorrelated scatterers, with the same density ρ, leads to a calculation of the average power in a fully disordered material $\langle P_a^U \rangle$ (we use the superscript U for quantities characterizing the uncorrelated material).

The dependence of $\langle P_a^H \rangle$ and $\langle P_a^U \rangle$ on the ISA absorption optical thickness L/ℓ_a^B is shown in Fig. 1 (a). The parameter $L/\ell_a^B = \rho\sigma_a L$ is chosen here as a measure of the intrinsic absorption level, independently of the spatial correlations in the medium. The power absorbed by the stealth hyperuniform material is substantially larger than that absorbed in the fully disordered material with the same density. As shown in Fig. 1 (b), we observe a maximum enhancement $\langle P_a^H \rangle / \langle P_a^U \rangle \simeq 1.8$ for a thickness $L \simeq \ell_a^B$.

The propagation regimes in the hyperuniform and disordered structures can be analyzed, in order to get physical insight into the mechanism responsible for the absorption enhancement. The effective scattering mean free path in the non-absorbing hyperuniform structure is estimated to be $\ell_s^H \geq 750\,\ell_s^B$, based on a computation of the average field inside the medium (see App. C). This confirms that hyperuniform correlations, with the set of parameters chosen in Fig. 1, lead to transparency by suppressing the scattered power [24]. Moreover, we have verified numerically that the fluctuations of the absorbed power also vanish (see App. D), so that error bars are not displayed in the figures for the sake of lisibility. We can conclude that the hyperuniform material in this regime behaves as an effective homogeneous and absorbing medium. Note that homogenization emerges here as a consequence of spatial correlations, without any change in the density of scatterers. The descprition of the effective medium has to go beyond standard approaches, such as the Maxwell-Garnett model. The average absorbed power can be calculated analytically considering a homogeneous slab, with a complex refractive index given by the effective refractive index of the hyperuniform structure, also deduced from the computation of the average field inside the slab (see App. E). The result of the analytical calculation is represented in Fig. 1 (a), and nicely fits the numerical simulation, confirming the picture of an homogenization process. Regarding the uncorrelated medium, scattering is not suppressed, but the absorption curve can be fairly reproduced using a Monte Carlo simulation of intensity transport, describing the multiple scattering process in a medium with an effective refractive index $n_{\text{eff}}^U = \sqrt{1 + \rho\alpha(\omega)}$,
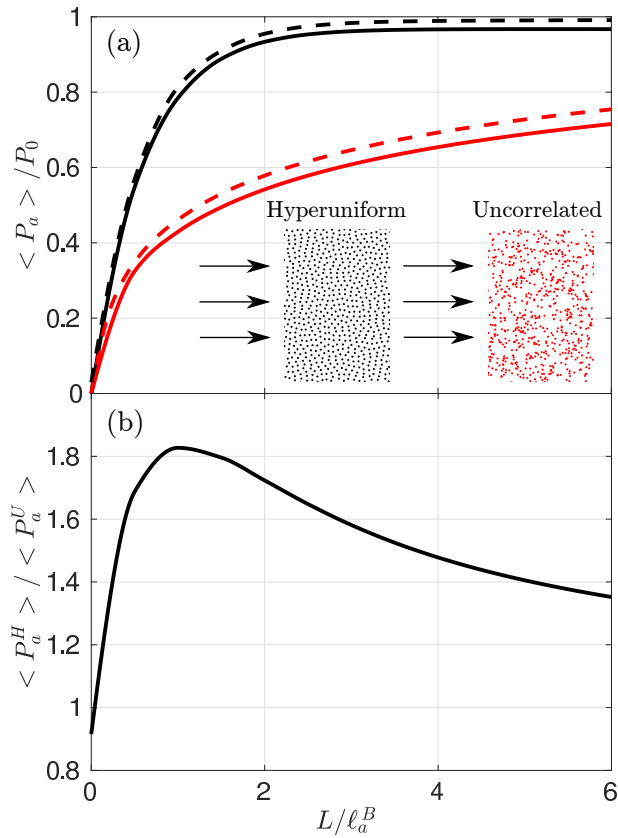
Fig. 1. (a) Normalized absorbed power averaged over 60 configurations, versus the ISA absorption optical thickness L/ℓ_a^B, for hyperuniform (black solid line) and uncorrelated (red solid line) materials. Parameters: $L/\ell_s^B = 15$, $k_0\ell_s^B = 13$, $N = 30000$ scatterers, $\chi = 0.44$. Black dotted line: absorption by a homogeneous material with a complex refractive index equal to the effective index of the hyperuniform material (obtained by a fitting procedure). Red dotted line: absorption by an uncorrelated medium computed using a Monte Carlo simulation. (b) Ratio $\langle P_a^H \rangle / \langle P_a^U \rangle$ measuring the absorption enhancement in the hyperuniform material.

and scattering and absorption mean-free paths $\ell_s^U = \ell_s^B$ and $\ell_a^U = \ell_a^B$, as shown in Fig. 1 (a). We have also verified using the Monte Carlo simulation that when $\ell_a^U \ll \ell_s^U$ the power absorbed by the uncorrelated structure approaches P_0. The reason is that most of the light is absorbed before being scattered.

Interestingly, although spatial correlations in the stealth hyperuniform structures have a huge impact on the scattering mean free path, they weakly affect the absorption mean free path. This result was already put forward in Refs. [27, 28] for hard spheres correlations, and is confirmed by numerical simulations for hyperuniform disorder (see App. F). Indeed, with the parameters used in Fig. 1, we have $\ell_a^H \simeq 0.7\ell_a^B$. This calls for a simple random walk picture, that explains qualitatively the behavior of $\langle P_a^H \rangle$ and $\langle P_a^U \rangle$. For the hyperuniform medium, we have $\ell_a^H \sim \ell_a^B < L \ll \ell_s^H$, meaning that the photons travel along the distance L without being scattered, with a high probability to be absorbed before escaping. For the uncorrelated medium, $\ell_s^U \sim \ell_s^B < \ell_a^U \sim \ell_a^B < L$, and a non-negligible fraction of photons are backscattered before being absorbed. These results are not specific to the value of χ that has been chosen. Since the absorption mean-free path weakly depends on χ, the results are valid as soon as the transparent

criterion is fulfilled [24].

From the validity of the intensity transport picture, we also expect the absorption enhancement to be robust against changes in the direction of incidence and the illumination frequency. This is confirmed by the dependence of $\langle P_a \rangle$ on the incidence angle θ_0 and the frequency ω displayed in Fig. 2. The dependence of $\langle P_a^H \rangle$ on θ_0 [Fig. 2 (a)] is weak (and weaker than that observed for $\langle P_a^U \rangle$), except at large angles where finite-size effects start to play an important role (the transverse size of the medium is limited to $3L$ in the simulation). Using broadband scatterers (quality factor $Q = 3$), we obtain a large absorption enhancement on a broad frequency range [Fig. 2 (b)]. The bandwidth with large absorption corresponds to the frequency range for which the condition $\ell_a^H \sim \ell_a^B < L \ll \ell_s^H$ remains satisfied. It is interesting to note that the disordered stealth hyperuniform material provides a maximum of absorption exceeding that obtained with a periodic crystal, together with a better angular robustness (numerical simulations for crystals are displayed in App. B).
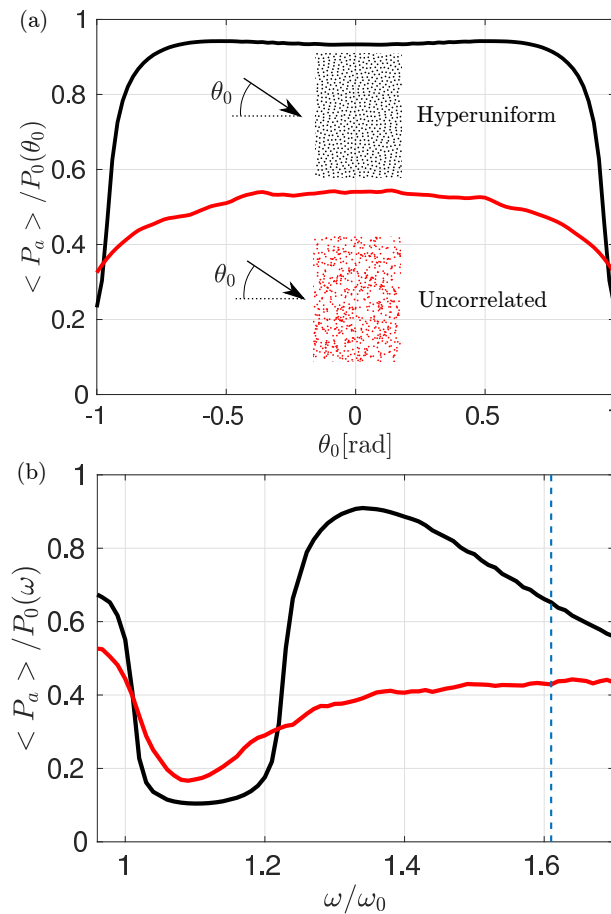

Fig. 2. (a) Normalized average absorption versus the angle of incidence. Same parameters as in Fig. 1 with $L/\ell_a^B = 2$. (b) Normalized average absorption versus the illumination frequency at normal incidence. Same parameters as in Fig. 1 with $Q = 3$ and $\eta = 0.94$ which gives $L/\ell_s^B = 15$, $L/\ell_a^B = 1$ and $k_0\ell_s^B = 13$ for $\omega/\omega_0 = 1.49$. The vertical dashed blue line indicates the cutoff frequency $\omega_c = Kc/4$ delimitating the transparency region $\lambda > 8\pi/K$.

Finally, it is interesting to use the analytical models to analyze the absorption enhancement at very large optical thicknesses, that are not accessible to the full-wave numerical simulation. For

the hyperuniform structure, we can calculate the power absorbed in an effective homogeneous slab with thickness L. We assume a dilute medium in order to neglect the index mismatch at the interfaces, and consider an absorption length $\ell_a^H \simeq \ell_a^B$ (see App. F). For the uncorrelated medium, we estimate the absorbed power using the diffusion approximation valid for $L \gg \ell_s^B$ (see App. G). Although not shown for brevity, the enhancement curves have the same shape as that in Fig. 1 (b), with an enhancement reaching $\langle P_a^H \rangle / \langle P_a^U \rangle \simeq 7$ for $L = 600\,\ell_s^B$ and $L \simeq \ell_a^B$. We can even estimate the maximum enhancement that can be expected using the analytical models (see App. H for details on the calculation). We obtain $(L/\ell_a^B)_{\text{optimum}} = 1.256$ and

$$\max\left[\frac{\langle P_a^H \rangle}{\langle P_a^U \rangle} \right] \simeq 0.243 \sqrt{\frac{L}{\ell_s^B}}. \tag{4}$$

4. Conclusion

In summary, we have demonstrated theoretically the existence of an upper bound for the absorbed power in a disordered medium, and analyzed the potential of hyperuniform materials for the design of strong absorbers of light. Hyperuniform correlations can enhance the absorbed power very close to the upper bound, and the non-resonant nature of the mechanism provides broad angular and spectral robustness. Robustness to positional variations of the scatterers is also expected, since random displacements do not seem to destroy hyperuniformity [48]. Together with the development of self-assembly processes able to produce hyperuniform architectures [49, 50], the results in this article could guide the design of disordered correlated materials with blackbody-like absorption. The results should apply to all kinds of waves propagating in materials made of subwavelength absorbing scatterers in a non-absorbing host medium.

A. Elements of multiple scattering theory in disordered media

Let us consider a random variable $\mathbf{X}$ for which a statistical average exists and is denoted by $\langle \mathbf{X} \rangle$. From that, we define the fluctuation $\delta\mathbf{X}$ for each statistical realization by the deviation to the average:

$$\mathbf{X} = \langle \mathbf{X} \rangle + \delta\mathbf{X}. \tag{5}$$

In the case of disordered media, this expansion can be applied for example to the electric field:

$$\mathbf{E}(\mathbf{r}, \omega) = \langle \mathbf{E}(\mathbf{r}, \omega) \rangle + \delta\mathbf{E}(\mathbf{r}, \omega) \tag{6}$$

where the statistics is performed here over all possible spatial configurations of the disordered medium. From this expansion, it is easy to compute the average intensity which reads

$$\langle I(\mathbf{r}, \omega) \rangle = \left\langle |\mathbf{E}(\mathbf{r}, \omega)|^2 \right\rangle = |\langle \mathbf{E}(\mathbf{r}, \omega) \rangle|^2 + \left\langle |\delta\mathbf{E}(\mathbf{r}, \omega)|^2 \right\rangle$$
$$= \bar{I}(\mathbf{r}, \omega) + \widetilde{I}(\mathbf{r}, \omega) \tag{7}$$

where we have used by definition $\langle \delta\mathbf{E} \rangle = \mathbf{0}$. $\bar{I}$ and $\widetilde{I}$ are respectively called the ballistic and the diffuse intensity. This expansion holds for any quadratic quantity such as the extinction, absorbed and scattered powers used in the main text:

$$P_e(\omega) = \frac{1}{2}\operatorname{Re}\int_V \mathbf{j} \cdot \mathbf{E}_0^* \mathrm{d}^3 r, \tag{8}$$

$$P_a(\omega) = \frac{1}{2}\operatorname{Re}\int_V \mathbf{j} \cdot \mathbf{E}^* \mathrm{d}^3 r, \tag{9}$$

$$P_s(\omega) = \frac{1}{2}\operatorname{Re}\oint_S (\mathbf{E}_s \times \mathbf{H}_s^*) \cdot \mathbf{n}_S \mathrm{d}^2 r. \tag{10}$$

We thus have

$$\langle P_e(\omega) \rangle = \overline{P_e}(\omega) + \widetilde{P_e}(\omega) = \overline{P_e}(\omega), \tag{11}$$

$$\langle P_a(\omega) \rangle = \overline{P_a}(\omega) + \widetilde{P_a}(\omega), \tag{12}$$

$$\langle P_s(\omega) \rangle = \overline{P_s}(\omega) + \widetilde{P_s}(\omega) \tag{13}$$

where we have used $\langle \mathbf{E}_0 \rangle = \mathbf{E}_0$ and $\delta \mathbf{E}_0 = \mathbf{0}$ since the incident field is deterministic.

A.1. Ballistic beam

From Eq. (7), we see that the ballistic intensity is directly given by the average field. Thanks to the multiple scattering theory, we can show that this field propagates in a homogeneous medium with an effective refractive index $n_{\mathrm{eff}}(\omega)$ [34, 35]. The imaginary part of this refractive index gives the attenuation of the average field as it propagates in the medium. This attenuation is called extinction and the typical distance over which the ballistic intensity is attenuated is the extinction mean-free path ℓ_e. We can also show that this attenuation is given by absorption (mean-free path ℓ_a) and losses by scattering (mean-free path ℓ_s). We have the relation:

$$\frac{1}{\ell_e} = \frac{1}{\ell_a} + \frac{1}{\ell_s}. \tag{14}$$

The different powers relative to the effective medium read:

$$\overline{P_e}(\omega) = \frac{1}{2} \operatorname{Re} \int_V \langle \mathbf{j} \rangle \cdot \mathbf{E}_0^* \mathrm{d}^3 r, \tag{15}$$

$$\overline{P_a}(\omega) = \frac{1}{2} \operatorname{Re} \int_V \langle \mathbf{j} \rangle \cdot \langle \mathbf{E}^* \rangle \, \mathrm{d}^3 r, \tag{16}$$

$$\overline{P_s}(\omega) = \frac{1}{2} \operatorname{Re} \oint_S [\langle \mathbf{E}_s \rangle \times \langle \mathbf{H}_s^* \rangle] \cdot \mathbf{n}_S \mathrm{d}^2 r \tag{17}$$

where

$$\langle \mathbf{j}(\mathbf{r}, \omega) \rangle = -i\omega \langle \mathbf{P}(\mathbf{r}, \omega) \rangle = -i\omega\epsilon_0 \left[n_{\mathrm{eff}}(\omega)^2 - 1 \right] \langle \mathbf{E}(\mathbf{r}, \omega) \rangle . \tag{18}$$

We also have

$$\overline{P_e}(\omega) = \overline{P_a}(\omega) + \overline{P_s}(\omega). \tag{19}$$

Equation (16) together with Eq. (18) are at the root of the computation of the absorbed power in the stealth hyperuniform medium (see App. E).

A.2. Diffuse beam

Regarding the computation of the diffuse intensity of Eq. (7), the problem is more complex. For large optical thicknesses, we can show that it is governed by a diffusion equation which is at the root of the computation of the absorbed power in the uncorrelated structure (see App. G).

B. Numerical computation of the average absorbed power

B.1. General method

The numerical computation is done through the following process schematized in Fig. 3. (1) First, we generate 20 disordered configurations containing 90000 points in a square of size $3L$. For the hyperuniform point patterns, we use the algorithm of Ref. [24] and uncorrelated point patterns are simply generated with a uniform random process. (2) To mimic a slab geometry and improve the statistical average, the generated configurations are divided into three bands of thickness L and length $3L$. After dressing all points with a polarizability $\alpha(\omega)$, Maxwell's

equations are solved in these configurations for a plane-wave illumination from the left and using a coupled-dipoles method [47]. In this formalism and for 2D scalar waves, the exciting field on scatterer i is given by

$$E_i(\omega) = E_0(\mathbf{r}_i, \omega) + k_0^2 \alpha(\omega) \sum_{j=1, j \neq i}^{N} G_0(\mathbf{r}_i - \mathbf{r}_j) E_j(\omega) \tag{20}$$

where E_0 is the incident field and G_0 is the Green function in vacuum. It connects the field to its point dipole source and is given by

$$G_0(\mathbf{r} - \mathbf{r}') = \frac{i}{4} H_0^{(1)}(k_0 |\mathbf{r} - \mathbf{r}'|) \tag{21}$$

where $H_0^{(1)}$ is the Hankel function of zero order and first kind. The computation of the exciting fields consists in solving the linear system given by Eq. (20). (3) Finally, to avoid finite-size effects again, the absorbed power is computed only for scatterers belonging to the central square of volume V using the relation

$$\frac{P_a}{P_0} = \frac{\sigma_a}{L|E_0|^2} \sum_{i \in V} |E_i|^2 \tag{22}$$

and a statistical average is performed using the 60 different realizations of the disorder to get $\langle P_a \rangle / P_0$.
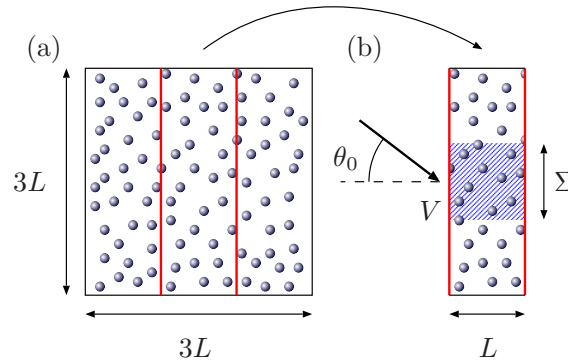

Fig. 3. Illustration of the numerical computation process. (a) Configuration generated numerically on a square of size $3L$ containing 90000 points. (b) One of the three bands used for the Maxwell simulation as a disordered pseudo-slab containing 30000 scatterers. The absorbed power is computed on the blue hatched square V. θ_0 is the angle of incidence of the plane-wave illumination.

B.2. Comparison with crystalline structures

We have also performed numerical simulations in the cases of fully ordered structures to compare with the hyperuniform and uncorrelated ones. The results are reported in Fig. 4. For the periodic lattices, the unit cell parameter a is such that $k_0 a = 1.95$ for the square lattice and $k_0 a = 2.10$ for the hexagonal lattice. This means that in both cases $a < \lambda$ and there is only one propagating Bloch mode (no Bragg peaks are visible). However, $\rho \lambda^2$ is not large enough for the crystalline structures to be homogenized (in the usual sense) and described by an effective refractive index. This makes the comparison to the hyperuniform structures difficult to address using simple arguments.
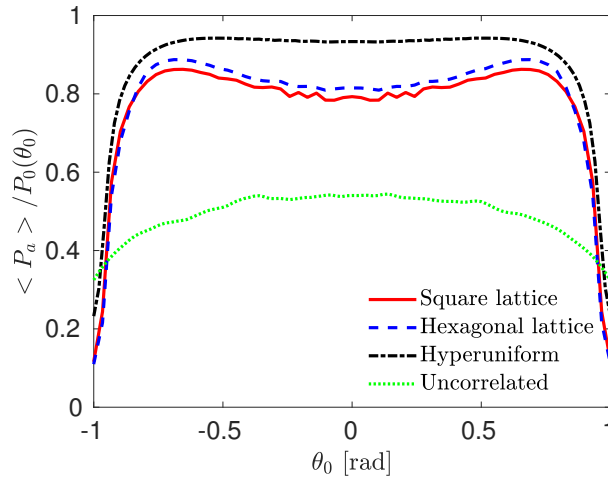
Fig. 4. Comparison of the power absorbed by different types of structures as a function of the incident angle θ_0. For all simulations, the geometry (slab), the number of scatterers and the optical properties of each scatterer are preserved. Parameters: $L/\ell_s^B = 15$, $L/\ell_a^B = 1$, $k_0\ell_s^B = 13$ and $N = 30000$ scatterers.

C. Average field evolution and effective refractive index fit for the stealth hyperuniform structure

To compute analytically the power absorbed by the stealth hyperuniform structures, we have to compute the evolution of the average field which allows us also to estimate the effective refractive index n_{eff}^H. The system of interest is depicted in Fig. 5. It is illuminated by a plane-wave at normal incidence given by
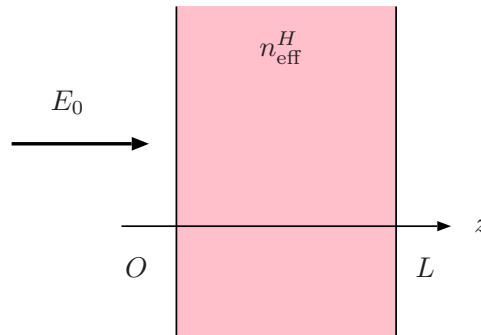
$$E_0(z) = E_0 \exp(ik_0z). \tag{23}$$

Fig. 5. System of interest to compute the average field (homogeneous slab).

First, we compute numerically the average field for several depths inside the slab. For that purpose, we compute for each configuration the field at any position using the expression

$$E(\mathbf{r}, \omega) = E_0(\mathbf{r}, \omega) + k_0^2\alpha(\omega) \sum_{j=1}^{N} G_0(\mathbf{r} - \mathbf{r}_j)E_j(\omega) \tag{24}$$

and the expressions of the exciting fields given by Eq. (20). Then we perform the statistical average. The numerical result is finally fitted with a standard Fabry-Perot approach which leads

to the theoretical expression of the average field given by

$$\langle E(z) \rangle = \frac{t}{1 - r_{\text{eff}}^{H\,2}} \left\{ \exp[ik_0(n_{\text{eff}}^H - 1)z] + \gamma \exp[-ik_0(n_{\text{eff}}^H + 1)z] \right\} E_0(z) \tag{25}$$

where $r_{\text{eff}}^H = r \exp(in_{\text{eff}}^H k_0 L)$, $\gamma = r \exp(2in_{\text{eff}}^H k_0 L)$, $r = (n_{\text{eff}}^H - 1)/(n_{\text{eff}}^H + 1)$ is the Fresnel amplitude coefficient in reflection and $t = 2/(n_{\text{eff}}^H + 1)$ is its counterpart in transmission. The fit is done using an optimization algorithm, based on a (global) genetic algorithm combined with a (local) Newton algorithm [51]. Note that in the most general case, the effective refractive index is non-local but it can be very well approximated by a simple complex constant for statistically homogeneous dilute systems.
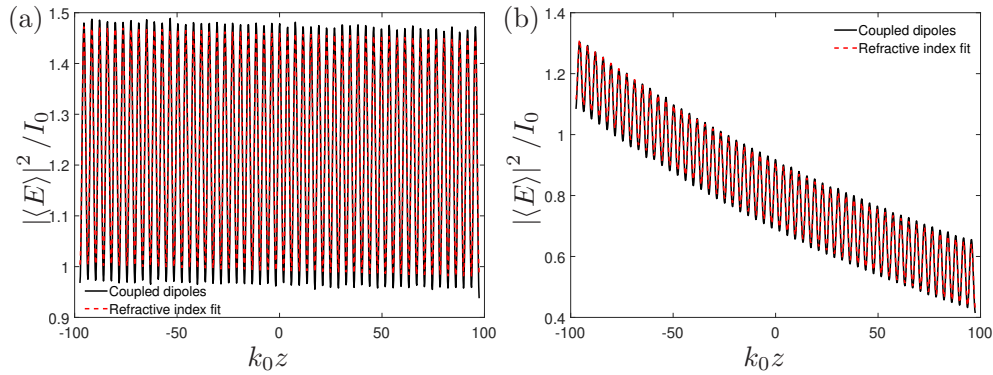

Fig. 6. Example of fitting of the effective refractive index of the average field inside the cloud. The average field is compared with the analytical solution of the field propagating inside an (transversally) infinite homogeneous slab of same refractive index. Calculations were done on 60 stealth hyperuniform configurations made of $N = 30000$ dipoles with $\chi = 0.444$, $L/\ell_s^B = 15$ and (a) $L/\ell_a^B = 0$ (no absorption) or (b) $L/\ell_a^B = 0.5$.

Figure 6 gives two examples for a stealth hyperuniform structure. From the effective refractive index, we get the extinction mean-free path by

$$\ell_e^H = \frac{1}{2k_0 n_{\text{eff}}^{H\,\prime\prime}} \tag{26}$$

where $n_{\text{eff}}^{H\,\prime\prime}$ is the imaginary part of the effective refractive index.

In Fig. 6 (a), there is no absorption and the extinction mean-free path can be assimilated to the scattering mean-free path. We clearly see the very slow decay of the intensity of the average field. which means that $\ell_s^H \gg L$ and the structure is transparent. The fit gives for Fig. 6 (a) $\ell_s^H \in [750, 1200]\ell_s^B$. This large window results from large incertaties because of a small decay. On the contrary, absorption is present in Fig. 6 (b). In that case, we cannot discriminate between the scattering and the absorption processes through the evolution of the average field. However, as pointed out in App. D, the fluctuations of the absorbed power vanish, which probably proves that ℓ_s^H remains large compared to the size of the system L. Thus the imaginary part of the refractive index gives here a direct access to the absorption length. The fit gives for Fig. 6 (b) $\ell_a^H \in [0.71, 0.83]\ell_a^B$. The proximity of ℓ_a^H with ℓ_a^B is surprising. It has already been put forward recently for a different correlation type (hard-sphere potential) [27, 28] and needs a more refined analysis that is left for future work. In particular, Eq. (22) could be used as a starting point for the derivation of a theoretical result regarding the expression of ℓ_a^H.

D. Standard deviation of the absorbed power distribution

To check the transparent character of the stealth hyperuniform structure for the set of parameters used in this work, we can compare the standard deviation obtained from the absorbed power distribution for both types of correlations (hyperuniform and fully disordered system). Figure 7 shows the computed ensemble standard deviation of the power absorbed σ_{P_a} relative to the ensemble mean power absorbed $\langle P_a \rangle$. It indicates clearly the strong reduction of σ_{P_a} for a stealth hyperuniform medium in the transparency regime, compared to an uncorrelated medium with the same intrinsic parameters, typically by one to two orders of magnitude. Furthermore, its amplitude in the hyperuniform case is more than two orders of magnitude smaller than $\langle P_a \rangle$, which indicates that $\langle P_a^H \rangle \simeq \overline{P}_a^H$. The power associated to absorption by the average field suffices to describe the absorption of a hyperuniform medium in the transparency regime for most applications. This relatively low standard deviation of the power absorbed is interpreted by the fact that a stealth hyperuniform medium in the transparency regime suppresses most of the ensemble fluctuations of the fields by definition of this regime. One may then expect that all the observables are described by the average fields. Note also that in the case of uncorrelated media, the larger the optical thickness L compared to ℓ_s^U, the closer $\widetilde{P}_s \to P_0$ and typically the larger $\sigma_{P_a^U}$ relatively to $\langle P_a^U \rangle$.
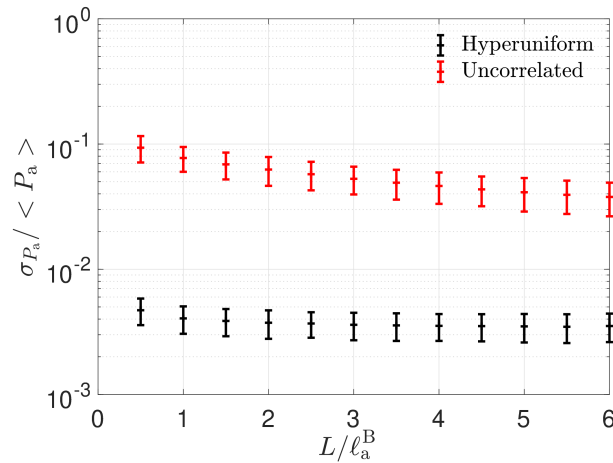

Fig. 7. Relative standard deviation of the absorption in a correlated (black, down) and uncorrelated (red, up) cloud. Same parameters as in Fig. 1 of the main text. Error bars were estimated by boostrapping on 10000 resampling and taking ±3 times the standard deviation obtained.

E. Average absorbed power for the stealth hyperuniform structure

Even in the presence of absorption, $\ell_s^H \gg L$ and the stealth hyperuniform structure remains transparent. This means that the fluctuations of the field vanish and $\widetilde{P}_s^H \ll P_0$ leading to $\langle P_a^H \rangle = \overline{P}_a^H$. Thus the power absorbed by the system is given by

$$\frac{\langle P_a^H \rangle}{P_0} = \frac{\omega}{2} \int \text{Im}[\langle P \rangle \langle E^* \rangle] dz \left[\frac{\epsilon_0 c I_0}{2} \right]^{-1} \tag{27}$$

where the average polarization field is given by $\langle P \rangle = \epsilon_0 [n_{\text{eff}}^{H\,2} - 1] \langle E \rangle$. Using Eq. (25), we easily obtain an analytical and exact expression of the power absorbed by the slab as a function of its size $k_0 L$ and effective refractive index n_{eff}^H. In order to get more physical insights into

the absorption in the slab, approximations are possible. Indeed, if the slab is large enough, i.e. $n_{\text{eff}}^{H}{}'' k_0 L \gg 1$, round trips are not allowed and a very good approximation of Eq. (25) is given by

$$\langle E(z) \rangle = t \exp(i k_0 n_{\text{eff}}^{H} z) E_0. \tag{28}$$

Using this expression in Eq. (27) leads to

$$\frac{\langle P_a^H \rangle}{P_0} = \frac{|t|^2}{2 n_{\text{eff}}^{H}{}''} \text{Im}\left[n_{\text{eff}}^{H\,2} \right] \left[1 - \exp(-2 k_0 n_{\text{eff}}^{H}{}'' L) \right] = [1 - R]\left[1 - \exp(-2 k_0 n_{\text{eff}}^{H}{}'' L) \right] \tag{29}$$

where $R = |r|^2$ is the factor of reflectivity in intensity of a single interface. We finally have

$$\frac{\langle P_a^H \rangle}{P_0} = [1 - R]\left[1 - \exp\left(-\frac{L}{\ell_a^H} \right) \right] \tag{30}$$

which is the expression used in Fig. 1 (a) of the main text (with a fitted refractive index).

F. Absorption mean-free path and hyperuniformity

Figure 8 shows the normalized average absorbed power of stealth hyperuniform clouds with different values of the parameters of interest such as the ISA optical thickness L/ℓ_s^B, the order degree χ, or disorder strength $k_0 \ell_s^B$.
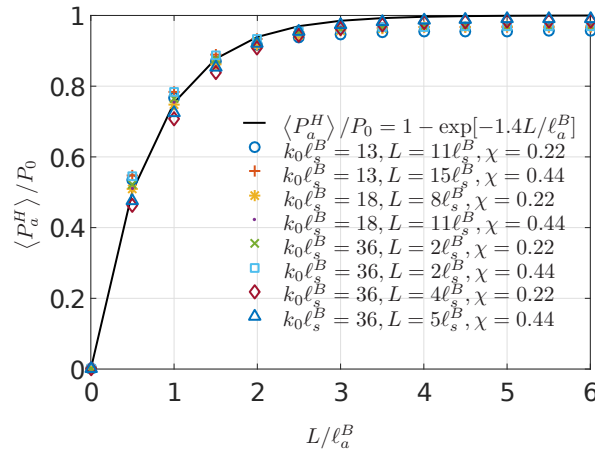

Fig. 8. Normalized average absorbed power for stealth hyperuniform structures operating in the transparent conditions showing weak variability of the absorption mean free path ℓ_a^H with the correlations.

As the extinction length is only given by the absorption length ℓ_a^H, the weak variability observed in the curves shows that ℓ_a^H is weakly affected by the presence of structural correlations. This is shown here for stealth hyperuniform media but it was already stressed for hard-spheres correlations [27, 28].

Nevertheless, a dummy fit by an exponential shows that the absorption mean free path deviates approximately by a factor $\ell_a^H/\ell_a^B \simeq 1/1.4 \simeq 0.7$ compared to the ISA absorption mean-free path and the normalized absorbed power is not exactly unity for very large absorption optical thickness. This comes from the fact that small corrections have to be taken into account due to the correlations in the scatterers positions, but also from the rather high density of scatterers (chosen due to computational constraints) and index mismatch at the interface [as shown by Eq. (30)].

For very dilute systems, the index mismatch can be neglected and assuming $\ell_a^H \sim \ell_a^B$, we obtain a simplified fully analytical expression for the average power absorbed by the hyperuniform structure given by

$$\frac{\langle P_a^H \rangle}{P_0} = \left[1 - \exp\left(-\frac{L}{\ell_a^B} \right) \right] \tag{31}$$

which is the expression used to evaluate the average absorption power in the stealth hyperuniform case of Fig. 9. Note that the assumption $\ell_a^H \sim \ell_a^B$ is a convenient approximation but is not strictly correct as specified above.

G. Average absorbed power for the uncorrelated structure

In this appendix, we derive an analytic expression of the average power absorbed by an uncorrelated cloud using the diffusion approximation. Compared to Monte Carlo simulations, the derivation leads to a simple formula of the estimated gain for very large optical thicknesses. The diffusion approximation is valid (1) whenever the size of the cloud L is much larger than the scattering mean-free path ℓ_s^B, (2) under the weak absorption condition $\ell_s^B \ll \ell_a^B$ and (3) in dilute systems such that $k_0 \ell_s^B \gg 1$. The system is considered diluted enough to neglect index mismatch at the interfaces and to set $\ell_s^U = \ell_s^B$ and $\ell_a^U = \ell_a^B$. Finally, as we consider uncorrelated point dipoles scatterers, the transport mean-free path is $\ell^* = \ell_s^B$. The diffusion equation for the 2D slab geometry and for a plane-wave illumination at normal incidence is given by [52]

$$\frac{c\ell_s^B}{2} \frac{d^2 \widetilde{u}}{dz^2} - \frac{c\widetilde{u}}{\ell_a^B} = -\frac{\overline{P}}{\ell_s^B} \tag{32}$$

where $\widetilde{u}$ is the energy density of the diffuse part of the beam and

$$\overline{P}(z) = P_0 \exp\left(-\frac{z}{\ell_e^B} \right) \tag{33}$$

is the ballistic source term. To take into account properly the boundary conditions, we use

$$\widetilde{u}(z = 0) - z_0 \frac{d\widetilde{u}}{dz}(z = 0) = 0, \tag{34}$$

$$\widetilde{u}(z = L) + z_0 \frac{d\widetilde{u}}{dz}(z = L) = 0, \tag{35}$$

where $z_0 / \ell_s^B = \pi/4$ is the 2D extrapolation length [35]. The solution of this set of equations reads

$$\widetilde{u} = \frac{P_0 \gamma}{c} \left[\alpha^+ \exp\left(\frac{z}{\ell} \right) + \alpha^- \exp\left(-\frac{z}{\ell} \right) - \exp\left(-\frac{z}{\ell_e^B} \right) \right] \tag{36}$$

where

$$\alpha^\pm = \left[\mp \left(1 + \frac{z_0}{\ell_e^B} \right) \left(1 \mp \frac{z_0}{\ell} \right) \exp\left(\mp \frac{L}{\ell} \right) \pm \left(1 - \frac{z_0}{\ell_e^B} \right) \left(1 \pm \frac{z_0}{\ell} \right) \exp\left(-\frac{L}{\ell_e^B} \right) \right]$$

$$\times \left[2 \left(1 + \frac{z_0^2}{\ell^2} \right) \sinh\left(\frac{L}{\ell} \right) + 2 \frac{z_0}{\ell} \cosh\left(\frac{L}{\ell} \right) \right]^{-1}, \tag{37}$$

$$\gamma = \frac{2}{1 + \ell_s^{B2}/\ell_a^{B2}} \tag{38}$$

and $\ell = \sqrt{\ell_a^B \ell_s^B / 2}$. The power absorbed by the slab is given by

$$\left\langle P_a^U \right\rangle = \frac{c}{\ell_a^B} \int_0^L \langle u(z) \rangle \, dz \tag{39}$$

where $\langle u(z) \rangle = \overline{u}(z) + \widetilde{u}(z)$ is the average energy density. We have $\overline{u}(z) = \overline{P}(z)/c$, thus we obtain

$$\frac{\left\langle P_a^U \right\rangle}{P_0} = \frac{\ell_e^B}{\ell_a^B} [1 - \gamma] \left[1 - \exp\left(-\frac{L}{\ell_e^B} \right) \right] + \frac{\ell}{\ell_a^B} \left\{ \alpha^+ \left[\exp\left(\frac{L}{\ell} \right) - 1 \right] + \alpha^- \left[1 - \exp\left(-\frac{L}{\ell} \right) \right] \right\} \tag{40}$$

which is the expression used to evaluate the average absorption power in the uncorrelated case of Fig. 9.

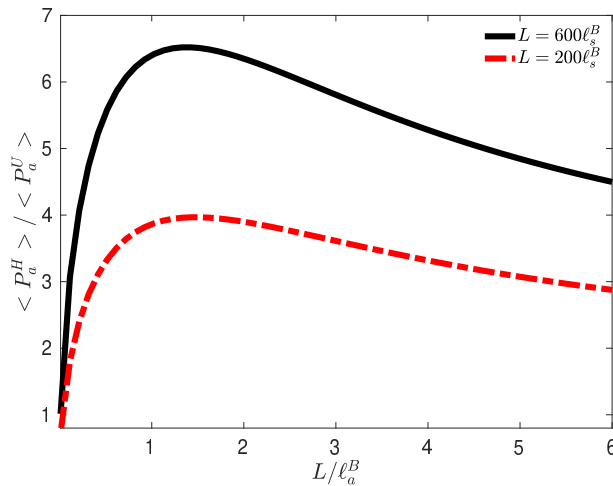## H. Estimation of the asymptotic maximum gain

Fig. 9. Estimated gain for large optical thicknesses.

To estimate the asymptotic maximum gain that we can get, we use Eq. (31) for the stealth hyperuniform structure. Regarding the uncorrelated system, we need to simplify Eq. (40) under the conditions $L/\ell_e^B \gg 1$, $L/\ell \gg 1$. By keeping only the second order terms of the expansion in ℓ_s^B/ℓ_a^B we obtain

$$\frac{\left\langle P_a^U \right\rangle}{P_0} = \left(1 + \frac{z_0}{\ell_s^B} \right) \sqrt{\frac{2\ell_s^B}{\ell_a^B}} - \left[1 + 2\frac{z_0}{\ell_s^B} \left(1 + \frac{z_0}{\ell_s^B} \right) \right] \frac{\ell_s^B}{\ell_a^B} + O\left(\frac{\ell_s^B}{\ell_a^B} \right). \tag{41}$$

The second term may be used to estimate the relative error commited by keeping only the first term. For instance, for $\ell_a^B = 40\ell_s^B$, the relative error is approximately 25 % and for $\ell_a^B = 240\ell_s^B$, the relative error is about 10 %. We then keep only the first term and we define the gain through the relation

$$G\left(\frac{L}{\ell_s^B}, \frac{L}{\ell_a^B} \right) = \frac{\left\langle P_a^H \right\rangle}{\left\langle P_a^U \right\rangle}. \tag{42}$$

The maximum gain is obtained when

$$\frac{\partial G}{\partial (L/\ell_a^B)} = 0 \tag{43}$$

which leads to

$$\left[\frac{L}{\ell_a^B}\right]_{\text{optimum}} = 1.256, \tag{44}$$

$$\max\left[\frac{\langle P_a^H \rangle}{\langle P_a^U \rangle}\right] \sim 0.243\sqrt{\frac{L}{\ell_s^B}}. \tag{45}$$

From this expression, we predict a gain of the order of 4 for $L = 200\ell_s^B$ and 7 for $L = 600\ell_s^B$ (see Fig. 9). It is important to note that Eq. (44) gives only an order of magnitude of the maximum gain and refinements are needed to be more accurate by taking into account the real effective refractive index for both the hyperuniform and the uncorrelated structures and the multiple scattering process beyond the diffusion approximation.

Funding

References

1. I. Sarbu and C. Sebarchievici, *Solar Heating and Cooling Systems* (Academic Press, Amsterdam, 2016).
2. A. Polman, M. Knight, E. C. Garnett, B. Ehrler, and W. C. Sinke, "Photovoltaic materials: Present efficiencies and future challenges," Science **352**, aad4424–1 (2016).
3. M. Osawa, *Surface-Enhanced Infrared Absorption Spectroscopy* (John Wiley & Sons, Ltd, 2006).
4. B. Sapoval, O. Haeberlé, and S. Russ, "Acoustical properties of irregular and fractal cavities," J. Acoust. Soc. Am. **102**, 2014–2019 (1997).
5. V. Leroy, A. Strybulevych, M. Lanoy, F. Lemoult, A. Tourin, and J. H. Page, "Superabsorption of acoustic waves with bubble metascreens," Phys. Rev. B **91**, 020301 (2015).
6. S. Brûlé, E. Javelaud, S. Enoch, and S. Guenneau, "Experiments on Seismic Metamaterials: Molding Surface Waves," Phys. Rev. Lett. **112**, 133901 (2014).
7. M. Benzaouia, G. Tokic, O. D. Miller, D. K. P. Yue, and S. G. Johnson, "From solar cells to ocean buoys: Wide-bandwidth limits to absorption by metaparticle arrays," arXiv 1804.00600 (2018).
8. M. Hutley and D. Maystre, "The total absorption of light by a diffraction grating," Opt. Commun. **19**, 431–436 (1976).
9. Y. Chong, L. Ge, H. Cao, and A. Stone, "Coherent Perfect Absorbers: Time-Reversed Lasers," Phys. Rev. Lett. **105**, 053901 (2010).
10. W. Wan, Y. Chong, L. Ge, H. Noh, A. D. Stone, and H. Cao, "Time-reversed lasing and interferometric control of absorption." Science **331**, 889 (2011).
11. Y. D. Chong and A. D. Stone, "Hidden Black: Coherent Enhancement of Absorption in Strongly Scattering Media," Phys. Rev. Lett. **107**, 163901 (2011).
12. C. W. Hsu, A. Goetschy, Y. Bromberg, A. D. Stone, and H. Cao, "Broadband Coherent Enhancement of Transmission and Absorption in Disordered Media," Phys. Rev. Lett. **115**, 223901 (2015).
13. S. F. Liew, S. M. Popoff, S. W. Sheehan, A. Goetschy, C. A. Schmuttenmaer, A. D. Stone, and H. Cao, "Coherent Control of Photocurrent in a Strongly Scattering Photoelectrochemical System," ACS Photonics **3**, 449–455 (2016).
14. E. H. Sargent, "Colloidal quantum dot solar cells," Nat. Photonics **6**, 133–135 (2012).
15. R. Mupparapu, K. Vynck, T. Svensson, M. Burresi, and D. S. Wiersma, "Path length enhancement in disordered media for increased absorption," Opt. Express **23**, A1472–A1484 (2015).
16. V. B. Koman, C. Santschi, and O. J. F. Martin, "Maximal absorption regime in random media," Opt. Express **24**, A1306 (2016).
17. W.-K. Lee, S. Yu, C. J. Engel, T. Reese, D. Rhee, W. Chen, and T. W. Odom, "Concurrent design of quasi-random photonic nanostructures," Proc. Natl. Acad. Sci. U.S.A. **114**, 8734–8739 (2017).
18. D. M. Maurice, "The structure and transparency of the cornea," J. Physiol. **136**, 263 (1957).
19. S. Fraden and G. Maret, "Multiple light scattering from concentrated, interacting suspensions," Phys. Rev. Lett. **65**, 512 (1990).
20. A. Yamilov and H. Cao, "Density of resonant states and a manifestation of photonic band structure in small clusters of spherical particles," Phys. Rev. B **68**, 085111 (2003).
21. L. F. Rojas Ochoa, J. M. Mendez Alcaraz, J. J. Sáenz, P. Schurtenberger, and F. Scheffold, "Photonic Properties of Strongly Correlated Colloidal Liquids," Phys. Rev. Lett. **93**, 073903 (2004).
22. M. Rechtsman, A. Szameit, F. Dreisow, M. Heinrich, R. Keil, S. Nolte, and M. Segev, "Amorphous Photonic Lattices: Band Gaps, Effective Mass, and Suppressed Transport," Phys. Rev. Lett. **106**, 193904 (2011).

23. G. M. Conley, M. Burresi, F. Pratesi, K. Vynck, and D. S. Wiersma, "Light Transport and Localization in Two-Dimensional Correlated Disorder," Phys. Rev. Lett. **112**, 143901 (2014).

24. O. Leseur, R. Pierrat, and R. Carminati, "High-density hyperuniform materials can be transparent," Optica **3**, 763–767 (2016).

25. L. S. Froufe Pérez, M. Engel, J. J. Sáenz, and F. Scheffold, "Band gap formation and Anderson localization in disordered photonic materials with structural correlations," Proc. Natl. Acad. Sci. U.S.A. **114**, 9570–9574 (2017).

26. K. Vynck, M. Burresi, F. Riboli, and D. S. Wiersma, "Photon management in two-dimensional disordered media," Nat. Mater. **11**, 1017–1022 (2012).

27. O. Leseur, "Diffusion, localisation et absorption de lumière en milieux désordonnés. Impact des corrélations spatiales du désordre," Ph.D. thesis, Université Pierre et Marie Curie (2016).

28. B. Wang and C. Zhao, "Effect of dependent scattering on light absorption in highly scattering random media," Int. J. Heat Mass Transf. **125**, 1069–1078 (2018).

29. M. Q. Liu, C. Y. Zhao, B. X. Wang, and X. Fang, "Role of short-range order in manipulating light absorption in disordered media," J. Opt. Soc. Am. B **35**, 504–513 (2018).

30. M. Florescu and G. Gkantzounis, "Hyperuniform disordered structures for enhanced light absorption (Conference Presentation)," in *Physics, Simulation, and Photonic Engineering of Photovoltaic Devices VII,* vol. 10527 (SPIE, 2018), p. 105270J.

31. J.-P. Hugonin, M. Besbes, and P. Ben Abdallah, "Fundamental limits for light absorption and scattering induced by cooperative electromagnetic interactions," Phys. Rev. B **91**, 180202 (2015).

32. O. D. Miller, A. G. Polimeridis, M. T. Homer Reid, C. W. Hsu, B. G. DeLacy, J. D. Joannopoulos, M. Soljačić, and S. G. Johnson, "Fundamental limits to optical response in absorptive systems," Opt. Express **24**, 3329 (2016).

33. J. D. Jackson, *Classical Electrodynamics* (John Wiley and Sons, New-York, 1962).

34. P. Sheng, *Introduction to Wave Scattering, Localization and Mesoscopic Phenomena* (Academic Press, New York, 1995).

35. E. Akkermans and G. Montambaux, *Mesoscopic Physics of Electrons and Photons* (Cambridge University Press, Cambridge, 2007).

36. B. van Tiggelen and A. Lagendijk, "Resonantly induced dipole-dipole interactions in the diffusion of scalar waves," Phys. Rev. B **50**, 16729–16732 (1994).

37. S. Torquato and F. H. Stillinger, "Local density fluctuations, hyperuniformity, and order metrics," Phys. Rev. E **68**, 041113 (2003).

38. M. Florescu, S. Torquato, and P. J. Steinhardt, "Designer disordered materials with large, complete photonic band gaps," Proc. Natl. Acad. Sci. U.S.A. **106**, 20658 (2009).

39. W. Man, M. Florescu, K. Matsuyama, P. Yadak, G. Nahal, S. Hashemizad, E. Williamson, P. Steinhardt, S. Torquato, and P. Chaikin, "Photonic band gap in isotropic hyperuniform disordered solids with low dielectric contrast," Opt. Express **21**, 19972 (2013).

40. N. Muller, J. Haberko, C. Marichy, and F. Scheffold, "Silicon Hyperuniform Disordered Photonic Materials with a Pronounced Gap in the Shortwave Infrared," Adv. Opt. Mater. **2**, 115–119 (2013).

41. M. Florescu, P. J. Steinhardt, and S. Torquato, "Optical cavities and waveguides in hyperuniform disordered photonic solids," Phys. Rev. B **87**, 165116 (2013).

42. W. Man, M. Florescu, E. P. Williamson, Y. He, S. R. Hashemizad, B. Y. C. Leung, D. R. Liner, S. Torquato, P. M. Chaikin, and P. J. Steinhardt, "Isotropic band gaps and freeform waveguides observed in hyperuniform disordered photonic solids," Proc. Natl. Acad. Sci. U.S.A. **110**, 15886 (2013).

43. T. Amoah and M. Florescu, "High-Q optical cavities in hyperuniform disordered materials," Phys. Rev. B **91**, 020201 (2015).

44. L. S. Froufe Pérez, M. Engel, P. F. Damasceno, N. Muller, J. Haberko, S. C. Glotzer, and F. Scheffold, "Role of Short-Range Order and Hyperuniformity in the Formation of Band Gaps in Disordered Photonic Materials," Phys. Rev. Lett. **117**, 053902 (2016).

45. O. U. Uche, F. H. Stillinger, and S. Torquato, "Constraints on collective density variables: Two dimensions," Phys. Rev. E **70**, 046122 (2004).

46. S. Torquato, "Hyperuniform states of matter," Phys. Rep. **745**, 1 (2018).

47. M. Lax, "Multiple Scattering of Waves. II. The Effective Field in Dense Systems," Phys. Rev. **85**, 621 (1952).

48. J. Kim and S. Torquato, "Effect of imperfections on the hyperuniformity of many-body systems," Phys. Rev. B **97**, 054105 (2018).

49. J. Ricouvier, R. Pierrat, R. Carminati, P. Tabeling, and P. Yazhgur, "Optimizing Hyperuniformity in Self-Assembled Bidisperse Emulsions," Phys. Rev. Lett. **119**, 208001 (2017).

50. P. M. Piechulla, L. Muehlenbein, R. B. Wehrspohn, S. Nanz, A. Abass, C. Rockstuhl, and A. Sprafke, "Fabrication of Nearly-Hyperuniform Substrates by Tailored Disorder for Photonic Applications," Adv. Opt. Mater. **6**, 1701272 (2018).

51. J. C. Spall, *Introduction to Stochastic Search and Optimization: Estimation, Simulation, and Control* (John Wiley & Sons, 2003).

52. A. Ishimaru, *Wave Propagation and Scattering in Random Media* (IEEE Press, Oxford, 1997).